FLASH FLOOD FORECASTING USING REMOTELY SENSED INFORMATION AND NEURAL NETWORKS PART II : MODEL APPLICATION

Gwangseob Kim[1] and Jong-Seok Lee[2]

[1]Department of Civil Engineering, Kyungpook National University, Taegu, Korea

[2]Utah Water Research Laboratory, College of Engineering, Utah State University, Logan, U.S.A.

Abstract: A developed Quantitative Flood Forecasting (QFF) model was applied to the mid-Atlantic region of the United States. The model incorporated the evolving structure and frequency of intense weather systems of the study area for improved flood forecasting. Besides using radiosonde and rainfall data, the model also used the satellite-derived characteristics of storm systems such as tropical cyclones, mesoscale convective complex systems and convective cloud clusters associated with synoptic atmospheric conditions as input. Here, we present results from the application of the Quantitative Flood Forecasting (QFF) model in 2 small watersheds along the leeward side of the Appalachian Mountains in the mid-Atlantic region. Threat scores consistently above 0.6 and close to 0.8 ~ 0.9 were obtained for 18 hour lead-time forecasts, and skill scores of at least 40 % and up to 55 % were obtained.

Key Words: Neural networks, Convective weather systems, Weather classifier, Flash flood forecasting, Hydroclimatology

1. INTRODUCTION

Along the Allegheny Front, in the mid- Atlantic region of the U.S. (Fig. 1), the hydroclimatology of floods is characterized by the recurrence of floods in small to medium watersheds. Such watersheds have a short response time for flooding, and are typically located in regions of complex orography, with narrow valleys and relatively strong relief. In this region, the character of the meteorological scenarios leading to severe flooding events differs between the warm (May through September) and cold (October through April) seasons. In the cold season, floods result from intense and/or lengthy rainfall on dense snowpacks or frozen ground. Here we focus on the wintertime storms that are generally associated with Pacific, Gulf and subtropical Atlantic moisture-rich airmasses. Often these watersheds are instrumented with streamflow gauges, but not with raingauges. At these locations, orographic effects on storm duration and intensity lead to the occurrence of heavy rainfall. These water-

sheds are connected through a dense network of 1st and 2nd order streams, which quickly deliver runoff from headwater catchments to the river valley downstream. When large storms impinge upon this region, the combined contribution of streamflow from these small basins to the main stem of the Susquehanna River leads to extreme floods (Barros and Kuligowski, 1998). Thus, the benefit of improving flood forecasting for such small basins is key to improve flood forecasting in the entire Susquehanna River basin.

To improve forecasting technique, we adopted an artificial neural network approach in this study. Previous studies have demonstrated that neural networks are appropriate to capture the complex nonlinear rainfall-runoff relationships (Hsu et al., 1995; Minns and Hall, 1996; Shamseldin, 1997; Campolo et al., 1999). The practical advantages and limitations of neural networks in forecast applications have been discussed by Maier and Dandy (1996) and Kuligowski and Barros (1998a,b) among others, while Hassibi et. al. (1994, 1995) demonstrated theoretically why neural networks are robust estimators of nonlinear phenomena. Also, neural networks have been applied to a wide variety of hydrologic problems such as precipitation forecasting (Kuligowski and Barros, 1998a,b; Hall et al., 1999); streamflow prediction (Imrie et al., 2000); and prediction of water quality parameters (Maier and Dandy, 1996) among others.

In this paper, we present results of application of the Quantitative Flood Forecasting (QFF) model which was developed to forecast peak streamflow in small size watersheds up to 18 hours in advance (Kim, submitted). The model consists of using neural networks as a data-transforming tool combining information from the state of the atmosphere and its recent evolution along with standard hydrometeorological data to issue streamflow forecasts. The structure of the model is dictated by our understanding of the regional hydrometeorology, flood hydrology and by an empirically derived classification that establishes relationships among data from different types of sensors: streamflow and rain gauges, radiosondes, and satellite imagery. Next , a description of the data used is provided in Section 2, which is followed by a brief review of the QFF model in Section 3. The application of the model is illustrated for two small watersheds in the mid-Atlantic region in Section using 18 hours forecast lead-times in Section 4. Final remarks and overall assessment of the approach are presented in Section 5.

2. DESCRIPTION OF DATA

2.1 Satellite Data and Characterization of Convective Weather Systems

The satellite data used to detect and monitor the presence of convective weather systems were obtained from the ISCCP-B3 data set (International Satellite Cloud Climatology Project; Rossow et al. 1987). The ISCCP-B3 data set provides cloud imagery with temporal resolution of 3 hours and spatial resolution of 30 kms. CCATS (Convection Classification and Automated Tracking System), an algorithm developed by Evans and Shemo (1996) to analyze infrared satellite data such as the ISCCP-B3, was used to detect, classify, and track the evolution of four different types of convective weather systems: tropical cyclones (CYC); mesoscale convective complexes (MCC); convective cloud clusters (CCC); and disorganized short-lived convection (DSL). The classification

criteria and the basic characteristics of each convective class are presented in Table 1. For this work, only five years of data between 1989 and 1993 were available, and Table 2 provides a summary of the basic statistics of the convective systems identified in this five-year period in our region of study. Note that, because the spatial resolution of the data is 30 kms and summertime thunderstorms in the mid-Atlantic region frequently occur at smaller spatial scales, the applicability of CCATS is limited to mesoscale convective activity during winter and spring. Furthermore, because of the small number of tropical cyclones (CYC), and because the convective cloud clusters (DSL) are typically very short-lived and thus not useful for long-time forecasts, only two of the convective classes were used in the QFF model development, specifically mesoscale complexes (MCCs) and convective clusters (CCCs). MCCs and CCCs are used in the QFF model as index variables that manifest the character of regional weather.

To illustrate the strong relationship between the presence of MCCs and rainfall production within an area, the relationship between MCC presence and associated streamflow and rainfall response are shown in Figs. 2. The solid line indicates the path of the MCC as it moves across our domain of study, and the colored dots are the rainfall rates measured at the raingauges in the radius of influence of the MCC trajectory. As the MCC evolves spatially over time, so does the number and locations where rainfall is observed. It should therefore be expected that by forecasting the trajectory of these systems, one should also be able to forecast the space-time evolution of rainfall across the landscape. To be used as input to the QFF model, the convective complexes and clusters were further classified as a function of the location of origin (i.e., where they are first detected) and direction of movement (i.e. direction of the trajectory). For this purpose, the region was subdivided in eight areas, and a spatial climatology of CCCs and MCCs was derived (Figs. 3(a)-(b)). The quadrants are classified clockwise from North as follows: 1- North; 2- Northeast; 3- East; 4- Southeast; 5- South; 6- Southwest; 7- West; 8- Northwest. Each class is defined for a range of 45° around the labeled direction [-22.5°, +22.5°]. Overall, convective systems move in the E-NE directions, and while MCCs originate mostly in W-SW-S-SE quadrants of the domain, CCCs originate mainly on the S-SE quadrants. This is consistent with the climatology of heavy rainstorms in the region, which are normally associated with southwesterly and southerly weather systems.

2.2 Radiosonde Data

Data from six radiosonde stations were used in this study (Tab. 3). Only directional wind data at 900 hPa, 850 hPa, 800 hPa , 750 hPa, 700 hPa, 650 hPa and 600 hPa pressure levels were used from each radiosonde station. Previous studies of the regional hydroclimatology of rain-producing weather systems in the Central Appalachian Mountains of the United States showed that northerly air masses generally do not cause rainfall in the region, and W-SW-S are prevailing wind directions for rain-producing weather systems (Barros and Kuligowski, 1996, 1998). In this study, the characteristics of wind direction for rain-producing weather systems are similar to that of previous research, and we used wind direction data to classify the weather conditions when convective activity was not detected by CCATS.

Table 1. Definitions and basic characteristics of conbvective weather systems from Satellite cloud imagery (Evans and Shemo, 1996)

Tropical Cyclones (CYC)	
Published storm tracks are used to validate storm tracks analyzed by CCATS.	
A tracking algorithm is used to follow the trajectory of tropical cyclones.	
Systems are matched with MCC or CCC tracks as defined below.	
Mesoscale Convective Complexes (MCC)	
Size	<-54°C region has area >50,000 km^2
Duration	>6 hours (2 frames in the case of ISCCP-B3)
Shape	Eccentricity (minor axis/major axis) > 0.7
Convective Cloud Clusters (CCC)	
Size	<-54°C region has area >4,000 km^2
Duration	> 6 hours (2 frames in the case of ISCCP-B3)
Shape	No shape criterion
Disorganized, Short-Lived Convection (DSL)	
Size	Temperature <-54°C for at least one pixel (i.e. Minimum size determined only by satellite resolution)
Duration	3 hours or less (1 frame in the case of ISCCP-B3)
Shape	No shape criterion

Table 2. Basic statistics of convective weather systems in our study region during 1989 - 1993

	CYC	MCC	CCC	DSL
Number	7	50	1,470	7,018
Average Life time (hours)	-	14	6	< 3
Area (km^2)	42,690	239,920	132,850	15,654
Temperature (K)	212	214	214	216
Eccentricity	0.75	0.70	0.53	0.61

Table 3. Radiosonde used in this study

Gauge ID	Name	Lat. (N)	Long. (W)	Elev. (m)
723270	Nashville metro. TN	6.08	-86.41	180
724030	Washington/Dulles, VA	38.57	-77.27	98
724250	Huntington/Tri stat, WV	38.22	-82.33	255
724290	Dayton/James M Cox, OH	39.54	-84.12	306
725200	Pittsburgh Intl, PA	40.30	-80.13	373
725280	Buffalo Intl Arpt, NY	42.56	-78.44	215

Table 4. Streamflow gauges used in this study

Name	Latitude (N)	Longitude (W)	Area (km^2)
Williamsburg	40.27	78.12	754
Loyalsockville	41.19	75.54	1,147

Table 5. Basic statistics of streamflow data from December to April between 1989 and 1993 periods

Name	Aver- (m^3/s)	Stdev (m^3/s)	Max. (m^3/s)	Percentile (m^3/s)				
				25	20 %	15 %	10 %	5 %
Williamsburg	18	21	268	20	23	27	35	51
Loyalsockville	33	43	673	39	45	54	65	90

Table 6. Summary of the different neural network configurations used in the QFF model

Model	Input Data Type
C4	Convective weather systems are present, and all predictor raingauges are wet.
C3	Convective weather systems are present, and more than 75% of predictor raingauges are wet.
R4	Convective weather systems have not been detected, and all predictor raingauges are wet.
R3	Convective weather systems have not been detected, and more than 75% of predictor raingauges are wet.
Combined	Various combinations of C4, C3, R4 and R3 based on data availability.

Table 7. Statistical performance measures of the QFF model for forecast lead-times of 18 hours [SS - skill score; CC - correlation coefficient; RMSE - root mean squared error. The threat scores are presented for 5 different streamflow percentiles (m^3/s).]

Name	Model	Tr#	RMSE (m^3/s)	SS	CC	Bias (m^3/s)	Threat Scores				
							25 %	20 %	15 %	10 %	5 %
Williamsburg	C4	10	11	0.96	0.97	3	0.79	0.94	1.00	1.00	0.71
	R4	10	33	0.62	0.72	-1	0.69	0.63	0.60	0.47	0.50
	R3	500	23	0.32	0.72	5	0.71	0.69	0.64	0.58	0.38
	Combined	-	23	0.54	0.75	3	0.72	0.71	0.67	0.60	0.44
Loyalsockville	C4	10	94	0.81	0.76	22	1.00	0.94	0.94	0.94	0.88
	R4	10	138	0.30	0.59	46	0.66	0.65	0.58	0.63	0.49
	R3	100	95	0.18	0.52	18	0.68	0.69	0.63	0.59	0.55
	Combined	-	88	0.39	0.65	11	0.69	0.69	0.64	0.61	0.61

2.3 Raingauge data

Hourly rainfall from 160 raingauges within the region (45N/85W ~ 33N/70W) were used in this study: 40 in New York- NY; 25 in Ohio-OH; 32 in Pennsylvania-PA; 3 in Maryland-MA; 9 in New Jersey-NJ; 3 in Kentucky-KT; 13 in West Virginia-WV; 16 in Virginia-VA; 3 in Tennessee-TN; 16 in North Carolina-NC. Missing data at these gauges were relatively small: in PA, WV, MD, NJ and VA, the rainfall data exceeded 90% reliability; in NY, OH, KT, TN and NC, the rainfall data exceeded 95% reliability.

2.4 Streamflow gauge data

Because hourly streamflow data are not available for West Virginia, 4 watersheds were selected in Pennsylvania with areal extent ranging from 750 km^2 to 1,150 km^2: Williamsburg and Loyalsockville (Tab. 4). The locations of the streamflow gauges corresponding to these watersheds are shown in Fig.1, while basic statistics of the streamflow data are provided in Table 5. The two watersheds selected have often experienced severe flooding in the past, and particularly in connection with major floods in the Susquehanna River basin (Barros and Kuligowski, 1998).

3. REVIEW OF THE QUANTITATIVE FLOOD FORECASTING MODEL

The QFF model consists of three different modules. In the first module, the raingauges are surveyed to look for rainfall occurrences. If no rainfall is detected in the study area, a no-rain forecast is issued. Next, the classification and decision module is used to describe and classify current synoptic atmospheric conditions using radiosonde and satellite data. A second rain/no rain forecast is issued based on the likelihood that rain may, or may not occur at the forecast locations within the prescribed lead-time (i.e. the next 18 hours). If a positive rain forecast is issued by the weather classifier, then the configuration of the neural network model will be selected according to the weather conditions (e.g. weather class, see Table 6) and as a function of input data available. Finally, the forecast module consists of a system of neural network models with at least four different configurations for each weather class. Hourly rainfall at four locations (i.e. predictor raingauges) and streamflow at the predicted gauge are respectively the inputs and outputs to the selected neural network model. The neural network output is an hourly streamflow forecast at the desired location at the desired time (desired time = current time + forecast lead-time).

In this study, the neural networks are composed of three layers including input layer, hidden middle layer, and output layer. Each node of the hidden layer receives a signal from every node in the input layer. Besides the data at the four predictor raingauges, the current streamflow is also used as input to the neural network model. Detailed description of the forecast model are presented in Kim (submitted).

4. RESULTS AND DISCUSSION

Table 6 provides a description of the four neural network model configurations used to issue four different types of forecasts in this study. These configurations were designed to reflect limitations associated with data availability and the type of forecast as well. The C4 configuration aims at forecasting the highest

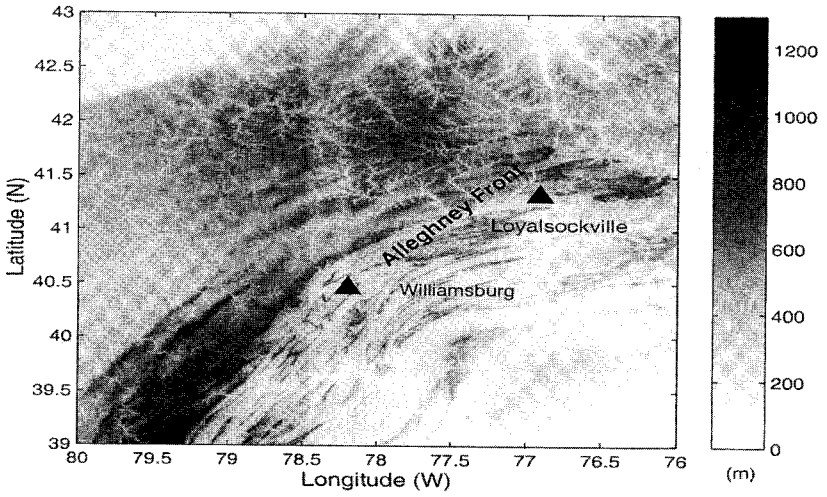

Fig. 1. The digital elevation map of Pennsylvania

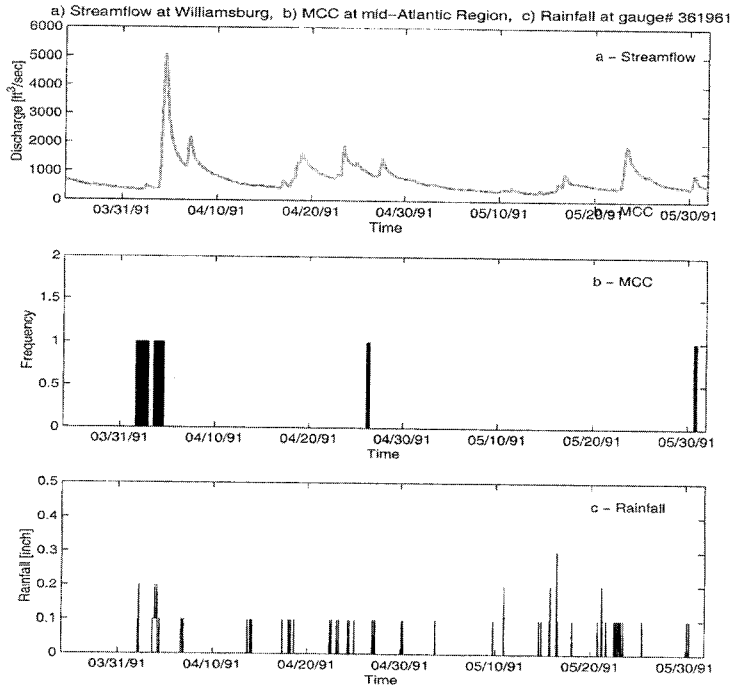

Fig. 2. The relationship between MCC presence and associated streamflow and rainfall response

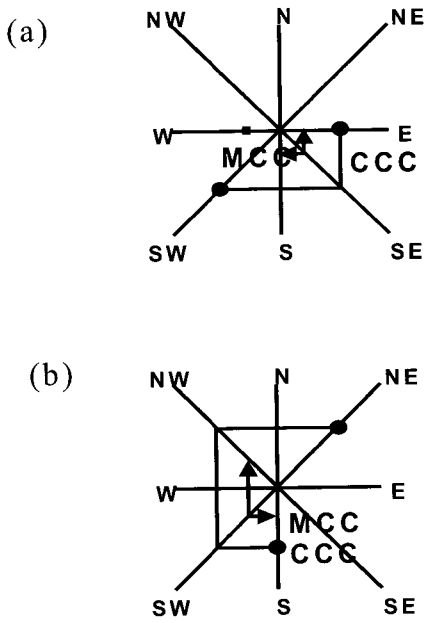

Fig. 3. Summary of the prevailing directional characteristics of convective weather systems: (a) origin and (b) moving direction

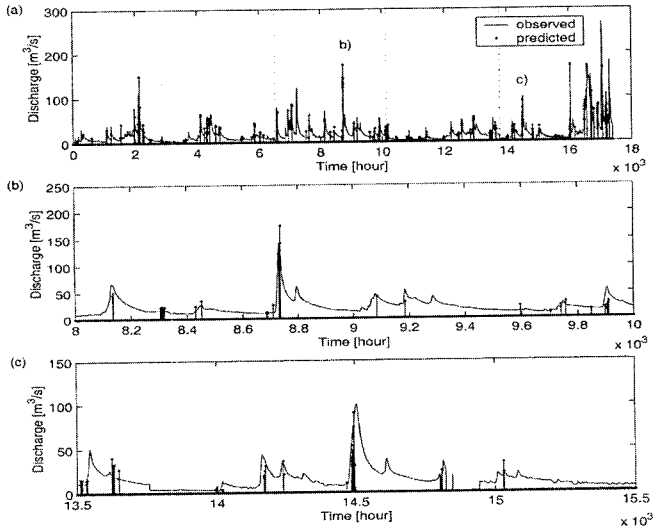

Fig. 4. (a) Time series of observed streamflow and the 18-hr lead-time combined forecasts at Williamsburg from December to April between 1989 and 1993 periods; (b) and (c) are enhanced zooms of short duration periods to illustrate model performance

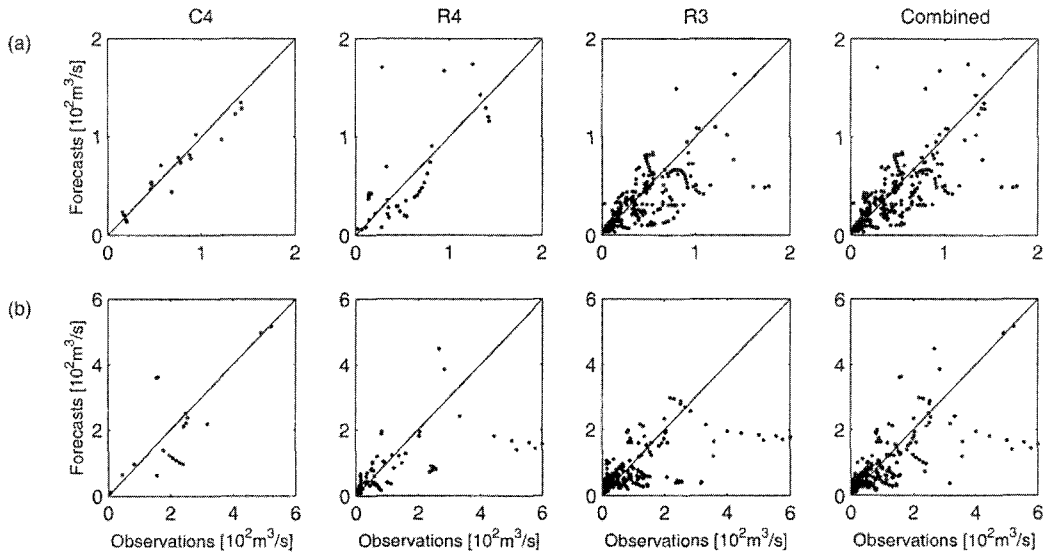

Fig. 5. Scatter plots of forecasted versus observed streamflow using four different types of 18-hr lead-time forecasts at the four study watersheds: (a) Williamsburg and (b) Loyalsockville

flood peaks, and can only be used if convective systems have been detected in the study region. The R4 configuration serves the same purpose of C4, but is used only when no convective systems have been detected. In the R3 configuration, only radiosonde data are used and forecasts are issued at all times. Thus, while the purpose of the C4 and R4 configurations is to capture the extremes, the purpose of the R3 configuration is to provide forecast coverage for all weather conditions. The combined forecast is a product obtained by selecting the highest forecast among C4, R4 and R3 outputs at all times.

Given that only five years of ISCCP-B3 data were available, model performance was evaluated using cross-validation to maximize the amount of data available for training: that is, the model was trained for each possible combination of four five-month periods (December-January-February-March-April), and the 5th was used to evaluate model performance. In this manner, performance statistics can be generated for the entire 5-year period.

The time series of observed hourly runoff amount and the combined forecast product is presented in Fig. 4(a), whereas Figs. 4(b)-(c) are zooms of the Fig.4(a) at different times to illustrate the overall quality of the QFF model performance. Overall, the figures show that peak streamflow values are captured well, and timing errors are small. A global evaluation of the individual flood forecasts is provided by the scatter plots in Figs.5(a) and (b), where the forecasts are compared with the observations on a

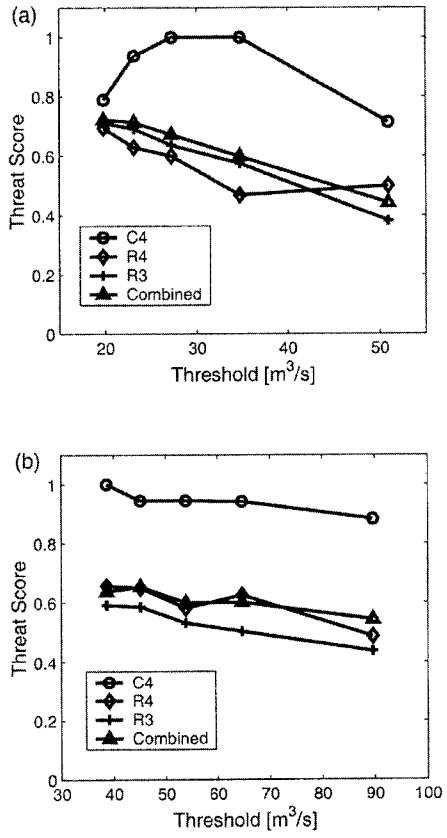

Fig. 6. Variation of threat scores for the 18 hour lead-time forecasts using the different neural network model configurations: (a) Williamsburg and (b) Loyalsockville. Thresholds are 25, 20, 15, 10 and 5 percentiles of streamflow for each location

one-to-one basis. Ideal forecasts should match the observations exactly, and therefore all the points in the scatter plot should fall on a 1:1 line. Remarkably, this is practically the case for the C4 forecasts. Note that although the C4 and the R4 configurations were developed with the same objective of capturing only the largest floods, the C4 forecasts follow the 1:1 line very closely, which illustrates the benefit of including the satellite data in the weather classification module operationally. Despite some false alarms (i.e. when the forecast significantly exceeds the observations) and forecast misses (i.e. when observed peaks are not captured), both of which are associated with timing errors, the model forecasts show very good agreement with the observed streamflow data for two basins.

Five quantitative measures of forecast skill were calculated to evaluate the model performance: 1) the skill score defined as the percentage

reduction in the mean-squared error with respect to persistence forecasting method; 2) the correlation coefficient, which describes the strength of the linear relationship between forecasts and observations; 3) the bias defined as the degree of correspondence between the mean forecast and the mean observation; 4) the root mean squared error defined as the sum of square of the differences of the forecasts and observations; and 5) the threat score, a categorical verification measure equal to the total number of correct event forecasts (hits) divided by the total number of flood forecasts plus the number of misses as used in Kuligowski and Barros (1998a) as follows:

$$threat = \frac{N_{hit}}{N_{obs} + N_{fct} - N_{hit}} \quad (1)$$

where N_{obs} is the number of observed amounts at or above a predetermined threshold; N_{fct} is the number of forecasts at or above this threshold; and N_{hit} is the number of instances where both forecast and the observation exceed the threshold.

A summary of the skill scores is provided in Tables 7 for 18 hours forecast lead-times. The skill scores are very high in comparison with the skill of Quantitative Precipitation Forecasts used to drive standard operational flood forecasting models, especially in the case of 18-hour lead-times. Again, especially remarkable are the skill scores obtained with the C4 configuration. To examine the results in more detail, Figs. 6(a) and (b) illustrate the variation in threat scores for the different model configurations and different thresholds, that is the 25th, 20th, 15th, 10th, and 5th streamflow percentiles. The real message implied by these results is that value-added forecasting skill by using the inherently synoptic and dynamical satellite data should not, and must not be ignored in operational flood forecasting. In addition, the performance of the QFF model was very similar for all four watersheds, showing that forecast skill is not sensitive to the spatial scale of the watershed upstream of the forecast location.

5. CONCLUSIONS

In this study, we developed an operational forecasting model for ungauged watersheds in the mid-Atlantic region using a data-driven approach which makes use of satellite, radiosonde, streamflow and rainfall data. This study validates our hypothesis that accurate and extended flood forecast lead-times can be attained if the synoptic evolution of atmospheric conditions is taken into consideration. Threat scores consistently above 0.6 and close to 0.8 ~ 0.9 were obtained for 18 hour lead-time forecasts, and skill scores of at least 20 % and up to 60 % were attained.

One contribution of this work is to demonstrate that multisensor data cast into an expert information system such as neural networks, if built upon scientific understanding of regional hydrometeorology, can lead to significant gains in the forecast skill of extreme rainfall and associated floods. While physically-based numerical weather prediction and river routing models cannot accurately depict complex natural non-linear processes, and thus have difficulty in simulating extreme events such as heavy rainfall and floods, data-driven approaches should be viewed as a strong alternative in operational hydrology. This is especially more pertinent at a time when the diversity of sensors in satellites and ground-based operational weather monitoring systems provide large volumes of data on a real-time basis.

REFERENCES

Barros, A.P. and Kuligowski, R.J. (1998). "Orographic effects during a severe wintertime rainstorm in the Appalachian Mountains." *Mon. Wea. Rev.*, Vol. 126, pp. 2468-2772.

Barros, A.P. and Kuligowski, R.J. (1996). "Quantitative precipitation forecasting issues in mountainous regions." *Proc. of the Int. Conf. on Water Resour. & Environ.* Res., (I), pp. 539-546.

Campolo, M., Andreussi, P., and Soldati, A. (1999). "River flood forecasting with a neural network model." *Water Resour. Res.*, Vol. 35, No. 4, pp. 1191-1197.

Evans, J.L. and Shemo, R.E. (1996). "Automated identification and climatologies of various classes of convection in the Atlantic Ocean." *J. Appl. Meteorol.* Vol. 35, pp. 638-652.

Hall, T., Brooks, H.E., and Doswell III, C.A. (1999). "Precipitation forecasting using a neural network." *Weather and Forecast.*, Vol. 14, pp. 338-345.

Hassibi, B., Sayed, A.H., and Kailath, T. (1994). "H^4 optimality criteria for LMS and backpropagation." *Adv. in Neural Info. Process.* Systems 6, pp. 351-359.

Hassibi, B. and Kailath, T. (1995). "H^4 optimal training algorithms and their relation to backpropagation." *Adv. in Neural Info. Process.* Systems 7, pp. 191-199.

Hsu, K.L., Gao, X., Sorooshian, S., and Gupta, H.V. (1997). "Precipitation estimation from remotely sensed information using artifical neural networks." *J. Appl. Meteorol.*, Vol. 36, pp. 1176-1190.

Imrie, C.E., Durucan, S., and Korre, A. (2000). "River flow prediction using artificial neural networks: generation beyond the calibration range." *J. Hydrol.*, Vol. 233, pp. 138-153.

Kim, G. (2001). "Flash flood forecasting using remotely sensed information and neural networks." Part I: model development, *J Civil Eng., KSCE*, submitted

Kuligowski, R.J. and Barros, A.P. (1998a). "Experiments in short-term precipitation forecasting using artificial neural networks." *Mon. Weather Rev.*, Vol. 126, pp. 470-482.

Kuligowski, R.J. and Barros, A.P. (1998b). "Localized precipitation forecasts from a numerical weather prediction model using artificial neural networks." *Weather and Forecast.*, Vol. 13, No. 4, pp. 1194-1204.

Maier, H.R. and Dandy, G.C. (1996). "The use of artificial neural networks for the prediction of water quality parameters." *Water Resour. Res.*, Vol. 32, No.4, pp. 1013-1022.

Minns, A.W. and Hall, M.J. (1996). "Artificial neural networks as rainfall-runoff models." *J. Hydrol. Sci.* Vol. 41, pp. 399-417.

Rossow, W.B., Kinsella, E., Wolf, A., and Garder, L. (1987). International satellite cloud climatology project description of reduced radiance data, *WMO TD-58*. World Meteorol. Org./Int. Council of Scientific Unions.

Shamseldin, A.Y. (1997). "Application of a neural network technique to rainfall-runoff modeling." *J. Hydrol.*, Vol. 199, pp. 272-294.

Department of Civil Engineering, Kyungpook National University, Taegu, Korea.
(E-mail : gskim@bh.knu.ac.kr)

Utah Water Research Laboratory, College of Engineering, Utah State University, Logan, USA.
(E-mail : slktf@usu.edu)